Dynamics and Structure Development during High Speed Melt Spinning of Nylon 6. I. On-Line Experimental Measurements

JAYENDRA H. BHEDA* and JOSEPH E. SPRUIELL, *Department of Materials Science and Engineering and Center for Materials Processing, University of Tennessee, Knoxville, Tennessee 37996-2200*

Synopsis

On-line experimental measurements of filament diameter, temperature, and birefringence as a function of distance from the spinneret were carried out during melt spinning of two nylon 6 resins of differing molecular weight. Filament tension was also measured. A rapid diameter attenuation or "necking" was observed in the spinline for both resins at take-up velocities above 6000 m/min. Evidence of crystallization in the spinline was also observed at these high spinning speeds. An analytical technique was used to extract apparent elongational viscosity for each resin and heat transfer coefficient for the melt spinning process from the experimental results.

INTRODUCTION

Melt spinning of synthetic filaments has long been a subject of both commercial and scientific importance. Because of this, the literature abounds with studies in which the final as-spun properties are investigated as a function of resin characteristics and processing conditions. Numerous other investigators have emphasized the dynamics, rheological, and heat transfer aspects of the process. In the mid 1970s Ziabicki[1] summarized the literature dealing with the experimental and theoretical framework of the process at that time. More recently there has been much interest in high speed spinning due to its potential for high productivity or because of special properties developed in filaments spun at high speeds.[2-14]

Among the previous investigations are several dealing with nylon 6,[3,4,6,11,15-19] including a recent study from our laboratory describing the effect of molecular weight on the structure and properties of high speed spun nylon 6 filaments.[11] The present investigation was undertaken, in part, in order to provide greater understanding of the earlier results. The overall approach taken was to make on-line measurements of diameter, temperature, and birefringence of the spinning filaments as a function of distance from the spinneret and to compare these results to computed profiles obtained from mathematical modeling. This paper, referred to as Part I, describes the experimental on-line measurements and their interpretation. A second paper, Part II, describes the mathematical simulation and its comparison to experiment.

*Present address: Allied Fibers, Technical Center, P.O. Box 31, Petersburg, VA 23804.

Journal of Applied Polymer Science, Vol. 39, 447–463 (1990)
 CCC 0021-8995/90/020447-17$04.00

On-line measurements give information about rate of filament drawdown, the location in the spinline, and the temperature at which crystallization and orientation develop, as well as other insights into the manner in which changes in the spinning and polymer variables affect the spinline dynamics and the structure development process. In addition, on-line measurements provide a means for evaluation of some important process parameters and physical properties of the resins that are needed for simulation of spinning conditions not studied by experiment. The next section describes a method for evaluation of two of these.

EVALUATION OF APPARENT ELONGATIONAL VISCOSITY AND HEAT TRANSFER COEFFICIENT

An "apparent elongational viscosity" of the resin can be evaluated as a function of temperature from on-line measurements made on the running spinline. The required data are the measurements of filament diameter and temperature as a function of distance from the spinneret coupled with a measurement of the spinline tension carried out at a position near the filament take-up device. The procedure discussed here was first described by George and Deeg.[20] The procedure is outlined in Figure 1. Experimental diameter and temperature profiles and the tension measured at the bottom of

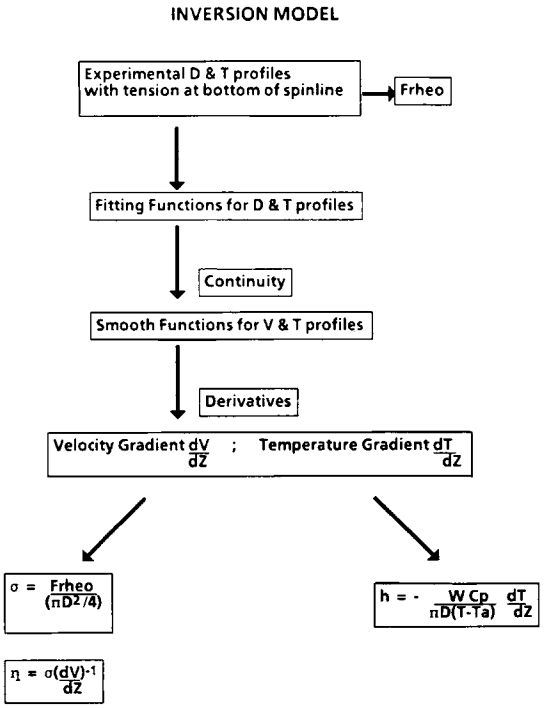

Fig. 1. Schematic of the procedure for computing the apparent elongational viscosity and heat transfer coefficient from experimental on-line measurements of spinline diameter, temperature, and tension.

the spinline are first used to compute the rheological force as a function of position along the spinline. The required calculation is an integration of the form

$$F_{\text{rheo}}(z) = F_L - \int_z^L \rho_{\text{air}} C_d V^2 \pi D \, dz - W[V(L) - V(z)]$$

$$+ \int_z^L \rho g \pi (D^2/4) \, dz \tag{1}$$

Here W is mass throughput, V is velocity, and F_L is the take-up tension for a spinline of length L. The density of the polymer melt, ρ, must be known as a function of temperature, and the calculation also requires a knowledge of the air drag coefficient C_d that determines the magnitude of the force component due to the air drag on the rapidly moving filament. The latter quantity has been evaluated by various investigators[21-25] and is known sufficiently accurately for take-up velocities less than 2000 m/min, where the air drag contribution is relatively small, so that little error is introduced by errors in the air drag coefficient.

Next the diameter and temperature profiles are fitted to smooth functions through regression analysis and the velocity profile is calculated using the continuity equation. The smooth velocity and temperature profiles are differentiated to obtain the velocity and temperature gradient profiles along the spinline. Combination of the rheological force and velocity gradient allows a calculation of the apparent elongational viscosity at each point along the spinline. In like manner, the temperature gradient profiles can be used to evaluate the heat transfer coefficient.

This approach can only be applied to smoothly varying diameter and temperature profiles and, hence, it is best applied in the absence of crystallization occurring in the spinline or to portions of the profiles that are not complicated by crystallization. In the case of nylon 6 crystallization does not occur on the spinline at spinning speeds below about 4000 m/min as we will show from our on-line measurements. Thus we were able to apply this procedure to on-line data for lower spinning speeds.

This approach would give the actual elongational viscosity if the polymer exhibited a Newtonian viscosity over the entire temperature range of measurement. In practice, most polymers exhibit non-Newtonian viscoelastic behavior and their viscosities depend on their deformation histories as well as their instantaneous deformation rates. However, for the case of nylon 6 we assume that the Newtonian approximation can be used, with caution, to obtain apparent elongation viscosities that can be used for comparison of various resins and for mathematical simulation.

EXPERIMENTAL

Materials and Melt Spinning

The two nylon 6 resins used in the present study had very different molecular weights as shown in Table I. These resins were also included in our earlier study of the effect of molecular weight on high speed spinning of nylon

TABLE I
Solution Viscosities of Nylon 6 Resins

Resin	Relative viscosity at 1.0 g/dL	Intrinsic viscosity	M_v
CN 9984	2.090	0.905	25,250
BHS	2.692	1.525	53,210

6, and more detail on these resins and the final structure and properties of filaments spun from them may be found in Ref. 11.

The equipment and procedures for melt spinning are also described in Ref. 11. Briefly, monofilaments were spun with an extrusion temperature of 260°C, nominal mass throughputs of 3 and 5 g/min, and take-up velocities in the range of 1000–7000 m/min. The filaments were spun into air at room temperature without crossblow and drawn down with a pneumatic drawdown device placed 2 m from the spinneret.

On-Line Measurement Techniques

Measurements carried out on the running spinline included diameter, temperature, and birefringence as a function of distance from the spinneret. The filament tension was also measured using a tensiometer located just above the drawdown device.

The diameter profiles were measured using a Zimmer diameter monitor which provides a noncontact technique for measurement of diameters up to 2 mm with a sensitivity of ± 0.5 μm. This monitor operates on an electrooptic back illumination principle that allows accurate measurements at filament linear velocities up to 10,000 m/min and lateral speeds of up to 500 m/min. The output from the diameter monitor was sent to a microcomputer for data storage and analysis. This allowed collection of large numbers of readings of diameter at each position along the spinline, statistical treatment of the data and plotting of the resulting distributions and profiles.

The birefringence profiles were measured using a microscope and compensator technique[14] to obtain the optical retardation. The microscope was mounted so that it could be easily moved up and down the spinline for on-line measurements. The retardation measurement at any position was divided by the diameter measured by the diameter monitor to obtain the birefringence.

A noncontact method using an infrared microscope system, the Barnes RM-2B, was used to measure the temperature profiles. The details of this measurement have been described elsewhere.[13,14]

RESULTS AND DISCUSSION

On-Line Measurements

The diameter distributions measured at 90 and 150 cm from the spinneret for sample CN9987 spun with 3 g/min throughput and a take-up velocity of 1960 m/min are shown in Figure 2. It is observed that the mean diameter

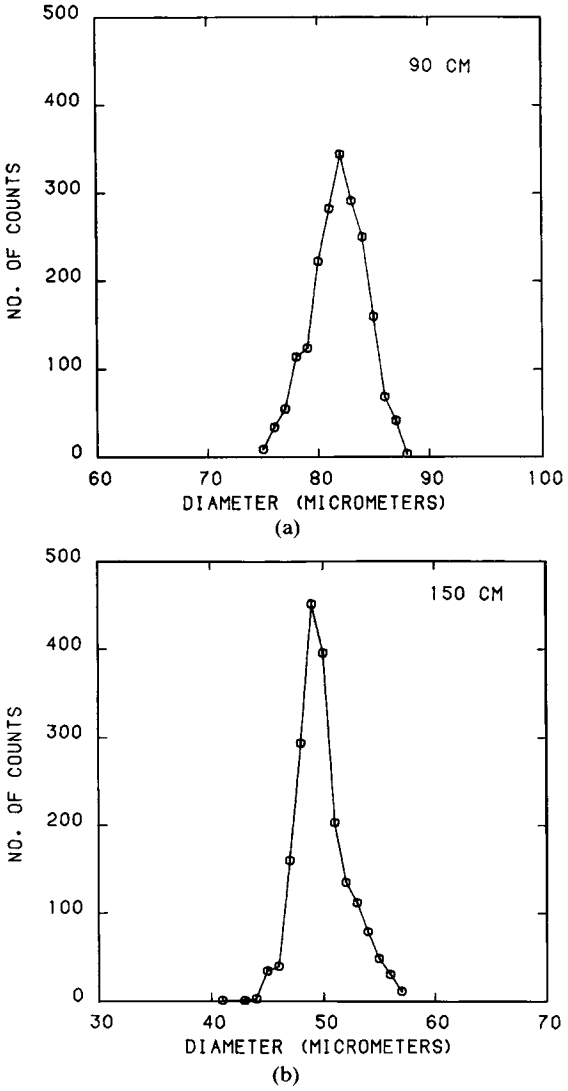

Fig. 2. Diameter distribution for CN9984 spun with a mass throughput of 3.07 g/min and take-up velocity of 1960 m/min: (a) 90 cm from spinneret; (b) 150 cm from spinneret.

decreases, as expected, and the distribution of diameters narrows as the distance from the spinneret increases. The bulk of the variation in diameters is likely to be associated with variations in the mass throughput W and take-up velocity V. Assuming this is true, an error analysis based on differentiation of the continuity equation shows that the relative error in the diameter is given by

$$\frac{\Delta D}{D} = \pm \frac{1}{2}\left(\frac{\Delta V}{V} + \frac{\Delta W}{W}\right) \tag{2}$$

This suggests that the variation in the diameter should decrease as the

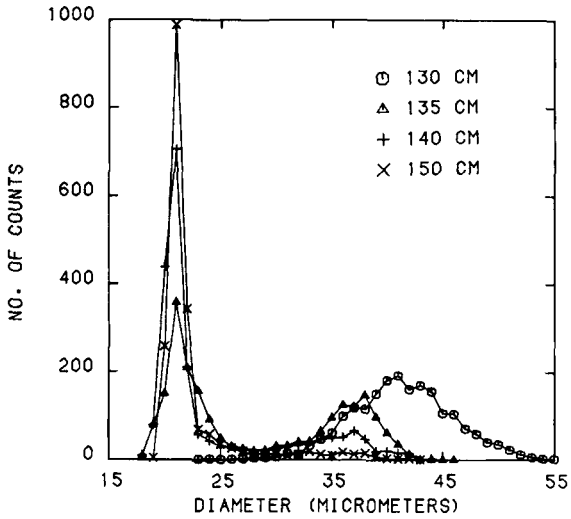

Fig. 3. Diameter distribution at the indicated distances from the spinneret for CN9984 resin spun with a mass throughput of 3.07 g/min and take-up velocity of 7310 m/min.

diameter decreases and the variation observed in Figure 2 is consistent with a sum of errors in the mass throughput and take-up velocities of order 10%. This seems reasonable due to the use of the pneumatic drawdown device for development and control of the take-up velocities; this method is known to be somewhat less accurate than the use of a constant speed godet roll.

Figure 3 shows the diameter distributions measured in the neighborhood of 140 cm from the spinneret at a much higher take-up velocity of 7300 m/min. At 130 and 150 cm from the spinneret the diameter distribution exhibits a single peak similar to those shown in Figure 2; but at 135 and 140 cm the distribution is bimodal. This behavior can be interpreted as resulting from the formation of a "neck" or sudden attenuation of the filament diameter. The position of the neck oscillates up and down the spinline by a few centimeters; this causes both the smaller diameter below the neck and the larger diameter above the neck to be recorded by the diameter monitor. Such necks have been previously reported for high speed spinning of polyesters.[2,10,13] The observation of the bimodal diameter distribution is a sure indication of the occurrence of such a neck. It is worth noting that the smaller diameter remains constant with a change in measurement position, indicating that further drawdown does not occur below the neck.

Examples of the mean diameter profiles are shown in Figure 4 for the CN9984 resin and in Figure 5 for the BHS resin. In Figure 4 it is observed that the necking is only observed at the highest spinning speed of 7300 m/min. At lower take-up velocities the filament diameter draws down gradually to its final value. It should be noted that the diameter values plotted at a position of 230 cm actually represent the final filament diameters measured off-line.

Neck formation was also observed for the BHS resin at high spinning speed and 3 g/min throughput [Fig. 5(a)]. At a mass throughput of 5 g/min necking was not observed in either resin in the range of take-up velocities investigated; this is shown for the BHS resin in Figure 5(b). The necking in diameter occurs

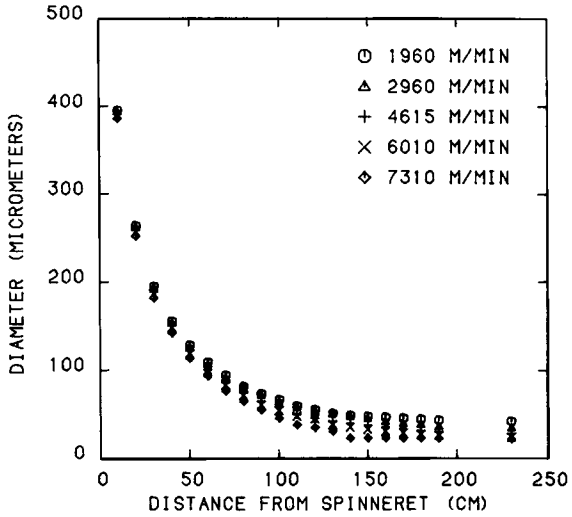

Fig. 4. Experimental diameter profiles for CN9984 resin spun with a mass throughput of 3.07 g/min.

at lower spinning speed and closer to the spinneret for BHS (6660 m/min and 115 cm) than for CN9984 (7300 m/min and 135 cm). This difference appears to be caused by the higher molecular weight of the BHS resin.

Birefringence and temperature profiles for the CH9984 resin are presented in Figure 6 while those for the BHS resin are shown in Figures 7 and 8. Birefringence is quite low near the spinneret but increases as the filament approaches its final diameter. Higher take-up velocities lead to higher final birefringence for a given resin and throughput. The rightmost points in the birefringence plots give the value of off-line birefringence measured as soon as possible after spinning. It required approximately 2 min after spinning to complete such a measurement.

Under spinning conditions that produce necking in the diameter profile, the birefringence rises rapidly in the region corresponding to the neck and approaches its final value well before the drawdown device is reached. The temperature profiles also show a slight plateau in the region near the neck. This observation is an indication that crystallization is occurring in the spinline when necking occurs.

It is well known that nylon 6 does not crystallize on the spinline at spinning speeds of the order of 1000 m/min or less, but it crystallizes on the take-up bobbin after spinning as it absorbs moisture from the surroundings. Previous researchers[3,4,6,11] studying high speed spinning have suggested that crystallization occurs in the spinline at sufficiently high spinning speeds. These suggestions are based on the aging behavior of as-spun filaments. Figure 9 shows the change in the birefringence of the present filaments with time after spinning. In the samples that did not exhibit necking in the spinline the birefringence increases substantially after a few minutes aging and then approaches a stable value. This effect is apparently caused by crystallization due to water absorption from the atmosphere. Note that in the cases where necking occurred at high spinning speed, there is no appreciable change of

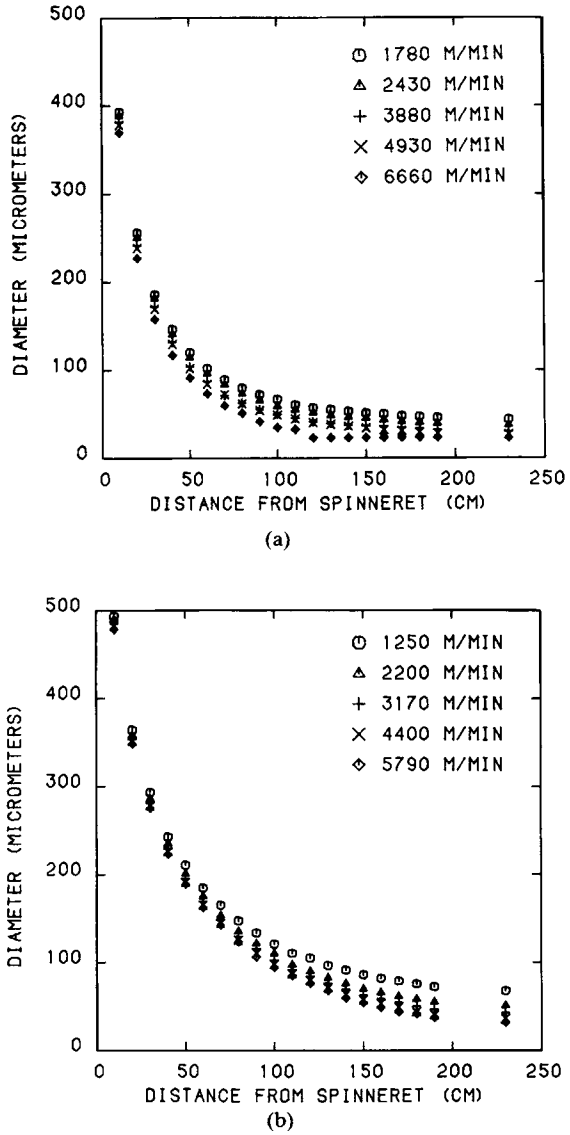

Fig. 5. Experimental diameter profiles for BHS resin: (a) mass throughput of 2.99 g/min; (b) mass throughput of 5.07 g/min.

birefringence with time after aging and the birefringence is stable at the value reached on the spinline. This further substantiates the suggestion that crystallization occurs on the spinline for those samples that exhibit necking.

Apparent Elongational Viscosity and Heat Transfer Coefficient

The apparent elongational viscosities of both resins were determined as a function of temperature using the inversion procedure described above. The technique was applied to the experimental diameter and temperature profiles measured for the lowest spinning speed at each mass throughput for each

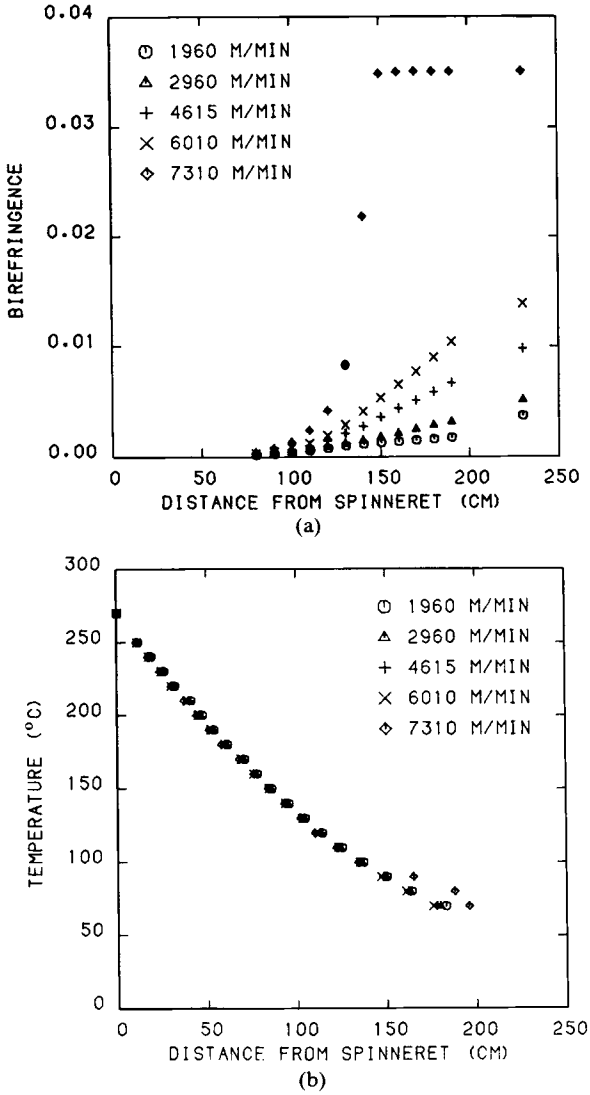

Fig. 6. On-line experimental measurements for CN9984 resin melt spun with a mass throughput of 3.07 g/min: (a) Birefringence profiles; (b) temperature profiles.

resin. These profiles were chosen in order to avoid any complications in carrying out the inversion procedure due to crystallization in the spinline.

The inversion procedure computes discrete values of the apparent elongational viscosity and heat transfer coefficient at specific points along the spinline. Figures 10 and 11 show an example of the results. In this figure the points plotted are the discrete values that result from the inversion procedure. The curves plotted through these discrete values represent the best fits obtained by regression analysis of eqs. (3) and (4), below, to the results:

$$\eta = B \exp(E/T) \tag{3}$$

$$h = k(V/A)^p \tag{4}$$

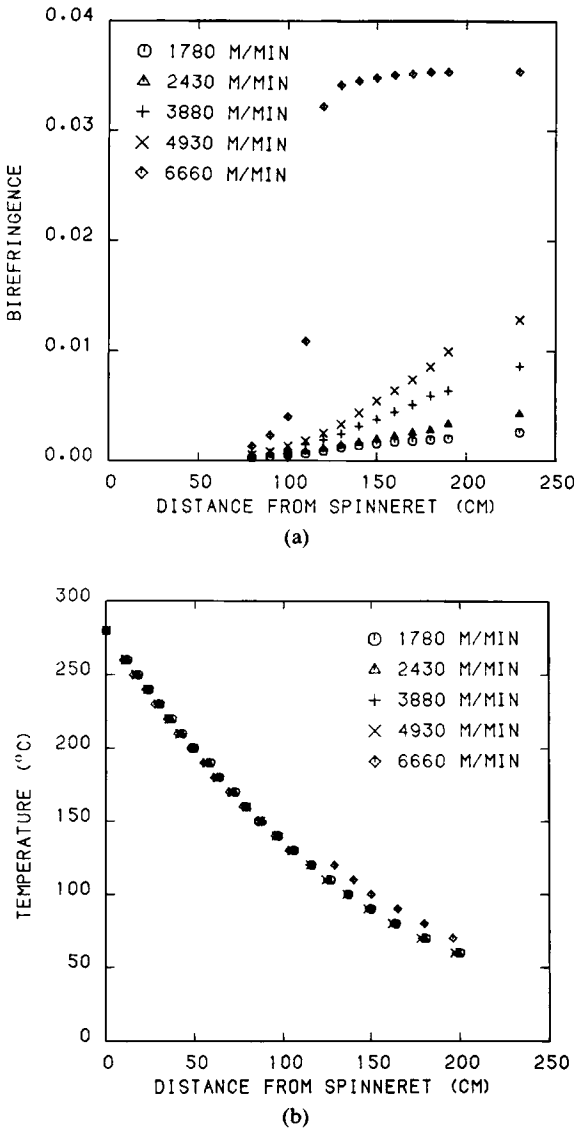

Fig. 7. On-line experimental measurements for BHS resin melt spun with a mass throughput of 2.99 g/min: (a) Birefringence profiles; (b) temperature profiles.

Equation (3) is the Arrhenius temperature dependence expected for viscosity. E is the activation energy for flow and T is the absolute temperature. Equation (4) is the form suggested by expressing the heat transfer relation of Kase and Matsuo[26] in terms of spinning variables. Here V is the local filament velocity and A is its cross-sectional area. In all of the present cases the apparent viscosities satisfactorily exhibited the expected Arrhenius temperature dependence while the heat transfer coefficients obeyed the power law dependence of eq. (4). We have also examined the sensitivity of the present results to potential errors in the correction factors used in computation of the rheological force, especially the air drag coefficient. For the present spinning

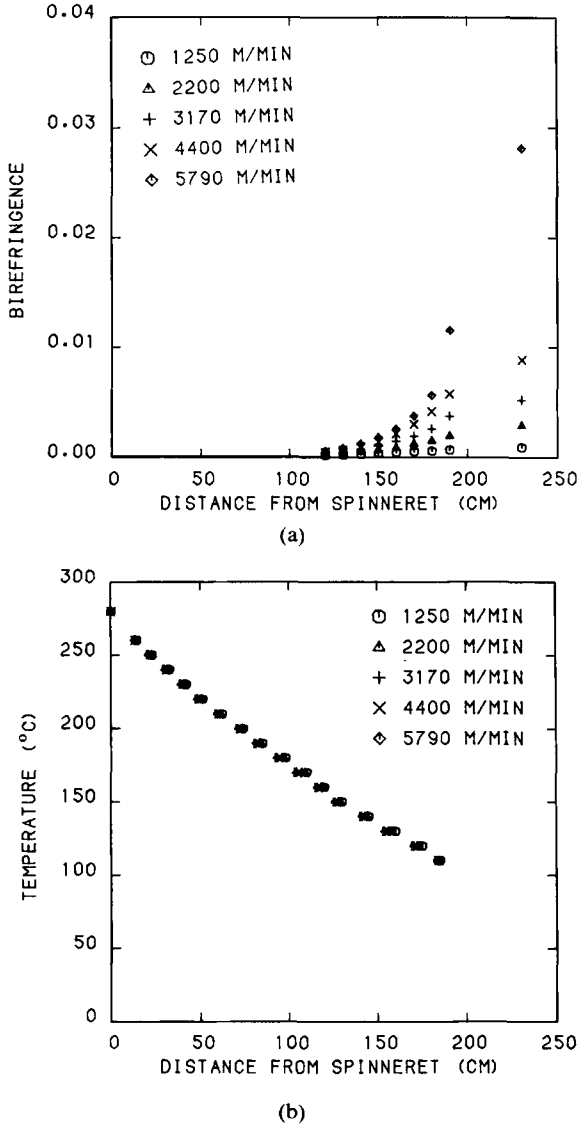

Fig. 8. On-line experimental measurements for BHS resin melt spun with a mass throughput of 5.07 g/min: (a) Birefringence profiles; (b) temperature profiles.

conditions the differences between results using the air drag correlation of Hamana et al.[15] and that of Sakiadis[22] was insignificant.

The values found for the constants in eqs. (3) and (4) for each resin and for each mass throughput examined are given in Table II. In the case of the apparent elongational viscosities, both the preexponential factor and the activation energy for flow are similar for each of the two different mass throughputs for each resin. Therefore, the data for both mass throughputs were combined and further regressed to a common equation for each resin. The resulting expressions for apparent elongational viscosity are for CN9984

$$\eta = 0.054 \exp(5140/T) \tag{5}$$

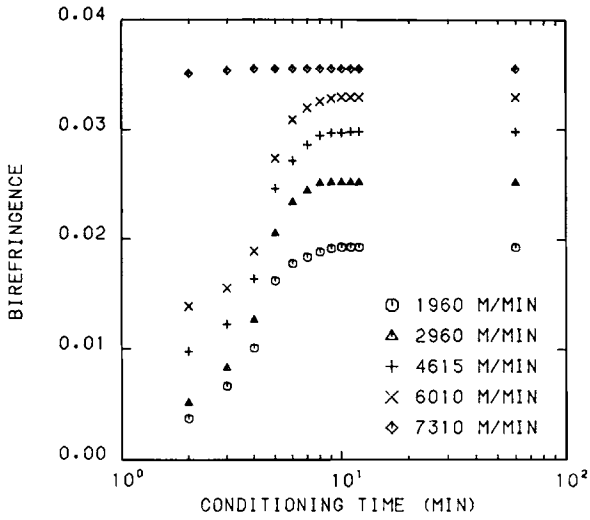

Fig. 9(a). Change in birefringence with conditioning time for CN9984 resin spun with a mass throughput of 3.07 g/min.

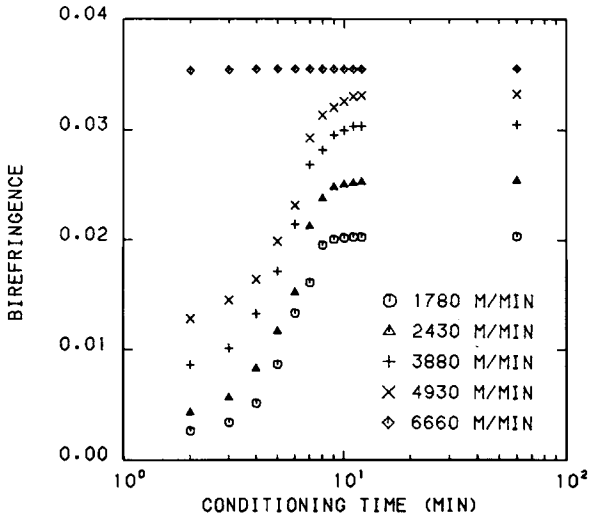

Fig. 9(b). Change in birefringence with conditioning time for BHS resin spun with a mass throughput of 2.99 g/min.

and for BHS

$$\eta = 0.092 \exp(5150/T) \tag{6}$$

The preexponential factor B clearly exhibits molecular weight dependence, but the activation energy for flow, E, appears to be independent of molecular weight in the range studied.

The values of the regression coefficients in Table II for the heat transfer coefficient are similar for both resins and for each mass throughput. This

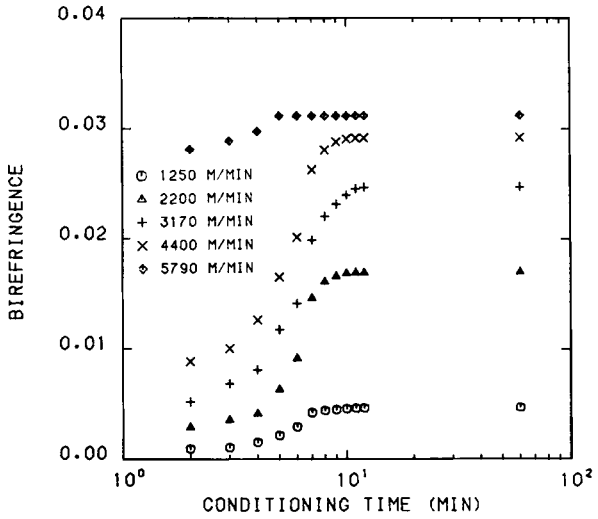

Fig. 9(c). Change in birefringence with conditioning time for BHS resin spun with a mass throughput of 5.07 g/min.

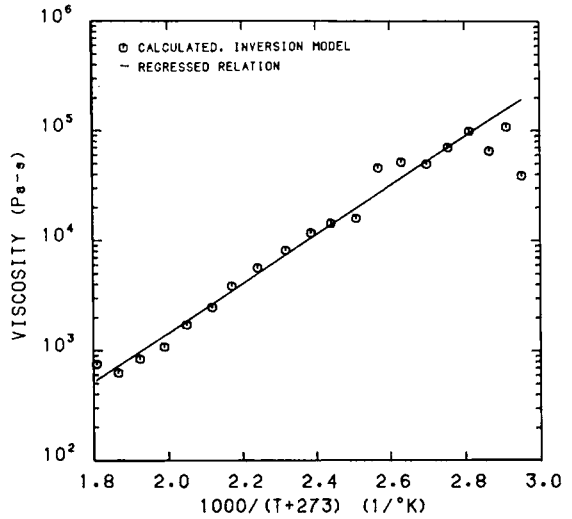

Fig. 10. Calculated and regressed viscosity relation from inversion procedure for CN9984 resin spun with a mass throughput of 3.07 g/min and take-up speed of 1960 m/min.

confirms that the heat transfer coefficient involved in melt spinning is not a material property. The heat transfer coefficient data for both mass throughputs and for both resins were combined and regressed to give the following overall equation:

$$h = 1.43 \times 10^{-4}(V/A)^{0.256} \tag{7}$$

There have been three previous studies in which measurements of elongational viscosities of nylon 6 were attempted. All of these studies used the melt

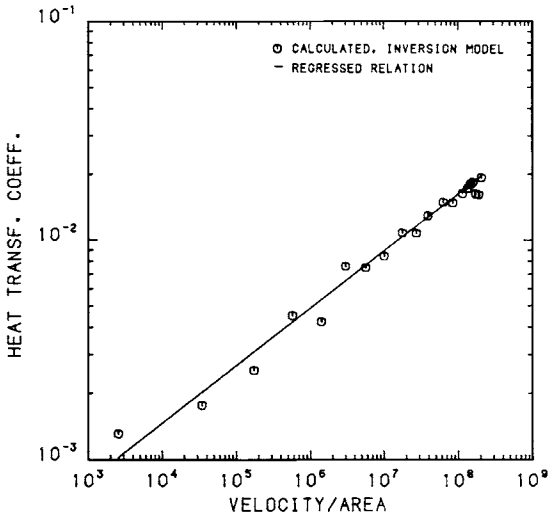

Fig. 11. Calculated and regressed heat transfer coefficient relation from inversion procedure for CN9984 resin spun with a mass throughput of 3.07 g/min and take-up speed of 1960 m/min.

TABLE II
Regression Coefficients for Apparent Elongational Viscosity and Heat Transfer Coefficient

Resin	Mass throughput (g/min)	Take-up velocity (m/min)	B (Pa s)	E (K)	k	p
CN 9984	3.07	1960	0.054	5149	1.32×10^{-4}	0.261
CN 9984	5.15	1570	0.047	5138	1.64×10^{-4}	0.249
BHS	2.99	1780	0.089	5140	1.38×10^{-4}	0.257
BHS	5.07	1250	0.093	5168	1.41×10^{-4}	0.258

spinning process as a basis for evaluation of elongational viscosity. Ishibashi et al.[16] studied four different nylon 6 resins with number average molecular weights in the range 18,500–24,100. They report that elongational viscosity was relatively independent of molecular weight and the take-up speed used in the melt spinning process, but that it was a strong function of temperature. The elongational viscosity values were consistently expressed by the equation

$$\eta = 33.32 \exp(3250/T) \tag{8}$$

Hamana et al.[15] studied a nylon 6 resin with a viscosity average molecular weight of 16,000, while Bankar et al.[18] studied a resin with a number average molecular weight of 23,000. We have regressed both of these results to an Arrhenius temperature dependence with correlation coefficients of 0.97 and 0.98, respectively.

In Figure 12 we compare the previous results to those found in the present investigation by plotting the regression equations for each result. We also plot an estimate based on our earlier shear data[11] for these same resins measured at

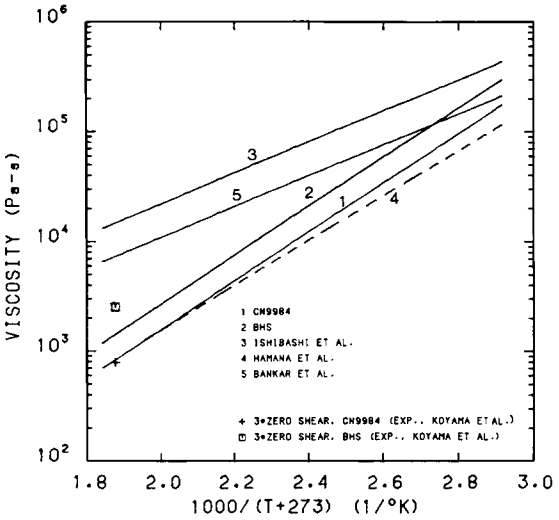

Fig. 12. Comparison of elongational viscosities from present inversion procedure with results from the literature.

a single temperature of 260°C. The "Trouton law" was used which states that the elongational viscosity is approximately three times the shear viscosity at very low shear rate.

The magnitudes of the present results at high temperatures are significantly lower than those of Ishibashi et al. and Bankar et al., but they do not seem out of line with the estimate based on shear data for the same resins or the data of Hamana et al. Further, the temperature dependence of the present results is similar to that of Hamana et al., but it is lower than the temperature dependence of shear data in the literature.[27,28] The reason for this is not clear at the present time. The experimental techniques used in the present study are significantly more accurate than those used in the early work of Bankar et al. This may be one of the primary reasons for the observed difference in temperature dependence.

The data obtained in the various studies have been obtained under different spinning conditions. This implies differences in elongation rates which might affect the results. This is also one of the major problems associated with the use of the melt spinning process to evaluate elongational viscosities as the elongation rate varies along the spinline. We do not believe this to be of major significance for the present results as use of the present results to simulate higher spinning speeds gave excellent comparisons with experimental data. These comparisons will be given in Part II; they indicate that the elongational viscosities of the present resins cannot be very sensitive to elongation rate.

The molecular weight dependence of the apparent elongational viscosity of nylon 6 does not seem quite as strong as that of the shear viscosity based on the present results. However, any detailed understanding of this behavior will require considerably more data than is presently available.

The results for the heat transfer coefficient are compared in Figure 13 with other reported correlations. Sano's[29] results are somewhat lower than the

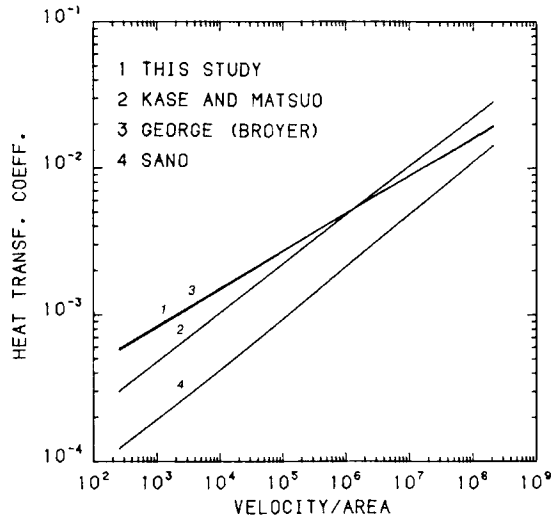

Fig. 13. Comparison of heat transfer coefficients from present inversion procedure with those from the literature.

present results but there is good agreement of the results of Kase and Matsuo,[30] Broyer,[31] and the present study. The excellent agreement of the present results with Broyer is perhaps fortuitous, but it may be remarked that Broyer is the only other result obtained from study of an actual spinline. The empirical relationship of Kase and Matsuo was developed using a stationary hot wire in an axial air stream, while Sano studied axial motion of a filament in stationary air.

CONCLUSIONS

The results of the present investigation led to several conclusions. In particular the on-line measurements verified earlier suggestions that crystallization of nylon 6 can occur in the spinline at sufficiently high take-up velocities. For the two resins studied, crystallization on the spinline was not clearly evident until spinning speeds exceeded 6000 m/min. At speeds below 6000 m/min, the filaments crystallized after spinning as they absorbed moisture from the environment. High spinning speeds produce high spinline stresses and increased molecular orientation which induces crystallization in the spinline. Increasing the molecular weight of the resin produces higher spinline stresses, due to higher elongational viscosity, and higher molecular orientation. This causes on-line crystallization to occur at a lower critical take-up velocity, with increased molecular weight. For given kinematic spinning conditions this leads to crystallization at higher temperature and closer to the spinneret with increasing molecular weight.

Rapid diameter attenuation or "necking" was observed in the spinline for nylon 6. This necking was only observed in cases where on-line crystallization was evident; consequently, it appears that the existence of necking is closely connected to the crystallization process in nylon 6.

An analytical technique was used to extract elongational viscosity and heat transfer coefficient data from the on-line diameter, temperature, and force

data. The heat transfer coefficient correlation was in good agreement with other results in the literature and seemed independent of material properties. The apparent elongational viscosities of the two resins studied exhibited an Arrhenius (exponential) temperature dependence and a molecular weight dependence that was somewhat weaker than expected based on shear viscosity data.

The authors thank Allied Fibers Division of Allied Signal, Inc. for support of this research and for permission to publish the results.

References

1. A. Ziabicki, *Fundamentals of Fiber Formation*, Wiley-Interscience, New York, 1976.
2. *High Speed Fiber Spinning*, A. Ziabicki and H. Kawai, Eds., Wiley-Interscience, New York, 1985.
3. H. M. Heuvel and R. Huisman, *J. Appl. Polym. Sci.*, **26**, 713 (1981).
4. H. M. Heuvel and R. Huisman, *J. Polym. Sci., Polym. Phys. Ed.*, **19**, 121 (1981).
5. J. Shimizu, N. Okui, and T. Kikutani, *Sen-i Gakkaishi*, **37**, T-135 (1981).
6. J. Shimizu, N. Okui, T. Kikutani, A. Ono, and A. Takaku, *Sen-i Gakkaishi*, **37**, T-143 (1981).
7. H. Yasuda, *Sen-i Gakkaishi*, **38**, P-154 (1982).
8. M. Matsui, *Sen-i Gakkaishi*, **38**, P-508 (1982).
9. H. H. George, A. Holt, and A. Buckley, *Polym. Eng. Sci.*, **23**, 95 (1983).
10. G. Vassilatos, B. H. Knox, and H. R. E. Frankfort, in *High Speed Fiber Spinning*, A. Ziabicki and H. Kawai, Eds., Wiley-Interscience, New York, 1985, p. 383; also G. Perez, *ibid*, p. 333.
11. K. Koyama, J. Suryadevara, and J. E. Spruiell, *J. Appl. Polym. Sci.*, **31**, 2203 (1986).
12. S. Chen and J. E. Spruiell, *J. Appl. Polym. Sci.*, **33**, 1427 (1987).
13. S. Chen, W. Yu, and J. E. Spruiell, *J. Appl. Polym. Sci.*, **34**, 1477 (1987).
14. Fu-Min Lu and J. E. Spruiell, *J. Appl. Polym. Sci.*, **34**, 1521, 1541 (1987).
15. I. Hamana, M. Matsui, and S. Kato, *Melliand Textilber.*, **4**, 382 (1969); **5**, 499 (1969).
16. T. Ishibashi, K. Aoki, and T. Ishii, *J. Appl. Polym. Sci.*, **14**, 1597 (1970).
17. T. Ishibashi and T. Ishii, *J. Appl. Polym. Sci.*, **20**, 335 (1976).
18. V. G. Bankar, J. E. Spruiell, and J. L. White, *J. Appl. Polym. Sci.*, **21**, 2341 (1977).
19. J. Gianchandani, J. E. Spruiell, and E. S. Clark, *J. Appl. Polym. Sci.*, **27**, 3527 (1982).
20. H. H. George and M. H. G. Deeg, paper presented at the second annual meeting of the International Polymer Processing Society, Montreal, Canada, 1986.
21. Y. Sano and K. Orii, *Sen-i Gakkaishi*, **24**, 212 (1968).
22. B. C. Sakiadis, *AIChEJ.*, **7**, 467 (1961).
23. Y. D. Kown and D. C. Prevorsek, *J. Appl. Polym. Sci.*, **23**, 3105 (1979).
24. J. Gould and F. S. Smith, *J. Text. Inst.*, **1**, 38 (1980).
25. M. Matsui, *Trans. Soc. Rheol.*, **20**, 465 (1976).
26. S. Kase and T. Matsuo, *J. Polym. Sci.*, **A3**, 2541 (1965).
27. G. Pezzin and G. B. Gechele, *J. Appl. Polym. Sci.*, **8**, 2195 (1964).
28. Z. Kemblowski and J. Torzecki, *Rheol. Acta*, **22**, 186 (1983).
29. Y. Sano, in *Formation of Fibers and Development of Their Structure*, The Society of Fiber Science and Technology, Ed., Japan, Kagaku Dojin, Kyoto, 1969.
30. S. Kase and T. Matsuo, *J. Polym. Sci.*, **3**, 2541 (1965).
31. H. H. George, *Polym. Eng. Sci.*, **22**, 292 (1982).

Received September 19, 1988
Accepted September 22, 1988